TOPICS IN LWS DATA ANALYSIS AND CALIBRATIONS*

M. Burgdorf[1], P. Clegg[2], D. Ewart[3,4], C. Gry[3,5], A. Harwood[3,4], S. Leeks[2], T. Lim[2,3], X. Liu[6], N. Minchin[2], P. Oldham[2], S. Pezzuto[3,7], S. Sidher[4,8], B. Swinyard[4], R. Sylvester[6], D. Texier[1], E. Tommasi[3], N. Trams[1]

[1]ISO Science Operations Centre, Astrophysics Division, Space Science Department of ESA, Villafranca, P O Box 50727, 28080 Madrid, Spain
[2]Queen Mary and Westfield College, University of London, Mile End Road, London E1 4NS, U K
[3]The LWS Instrument-Dedicated Team, ISO Science Operations Centre, P O Box 50727, 28080 Madrid, Spain
[4]Space Science Department, Rutherford Appleton Laboratory, Chilton, Oxon OX11 0QX, U K
[5]Laboratoire d'Astronomie Spatiale, BP 8, 13376 Marseille Cedex 12, France
[6]Department of Physics and Astronomy, University College London, Gower Street, London WC1E 6BT, U K
[7]Dip. di Fisica, Uni. di Lecce, CP 193, I-73100 Lecce, Italy
[8]Astrophysics Group, Blackett Lab, Imperial College , London, SW7 2BZ, U K

ABSTRACT

The strategy followed in the calibration of the LWS is briefly described and its fundamental results are reported. Routine measurements that were repeatedly done during the two years in orbit show that a reliable and stable mode of operations with high calibration accuracy has been achieved. In the course of the instrument running in space, however, also some unexpected problems were discovered. They were characterized with specific measurements and their impact on the instrument performance and consequences for data analysis are discussed. It is explained to which extent the undesirable effects could be corrected for by new procedures or modifications in the automatic processing. We deal in particular with the questions which targets and instrument modes require special attention by the observer and what further processing beyond the auto analysis stage is desirable or even necessary.

Key words: data processing; far infrared; space.

1. INTRODUCTION

The Long-Wavelength Spectrometer (LWS, Clegg 1996) operates in the far infrared band between 43 μm and 197 μm. Its resolving powers vary between 150 and 330 in grating mode and between 6800 and 9700 in Fabry-Perot (FP) mode. The infrared radiation is detected with photoconductive detectors made of doped-germanium, whose photocurrents are integrated at the input nodes of JFET amplifiers (Delettrez 1994). An astronomer defines his observations by use of four Astronomical Observing Templates (AOT's) which represent the different observing modes: line scan and wavelength range scan in grating and FP mode. The telemetry data from the satellite for these standardized observing modes are automatically processed in the Ground Station in Villafranca, and three product levels are generated: Edited Raw Data (ERD), Standard Processed Data (SPD) and Auto Analysis Results (AAR). Two software packages have been developed in order to further examine and process the pipeline products: the ISO Spectral Analysis Package (ISAP) and the LWS Interactive Analysis (LIA).

2. WAVELENGTH CALIBRATION

2.1. Grating Mode

The wavelength calibration for the LWS was done with end-to-end grating scans on targets with strong, well known lines. The wavelength standards used were mainly planetary nebulae like NGC6543 and H II regions. They provided seven different lines spread between 51 μm and 158 μm which appeared usually in more than one detector. The measurements showed that the relationship between commanded position of the grating in engineering units and its angle is very linear, especially in the central part of the scan range. Therefore fitting it with a polynomial produces very small coefficients for the higher terms and allows an interpolation for any wavelength with an accuracy better than a quarter of a resolution element. The resolution of the grating was found to be nominal with 0.29 μm in the short wavelength region and 0.6 μm in the long wavelength region.

*The LWS is part of ISO, an ESA project with instruments funded by ESA Member States (especially the PI countries: France, Germany, the Netherlands and the United Kingdom) and with the participation of ISAS and NASA.

The wavelength calibration of the grating has been checked for 20 months during routine phase with weekly end-to-end grating scans of planetary nebulae. It was found not to be perfectly stable; a little jump happened in revolution 346 (see figure 1). The size of this jump is bigger the farther the grating is situated away from its rest position in the center of the scan range, but even in the worst case it is less than half a resolution element.

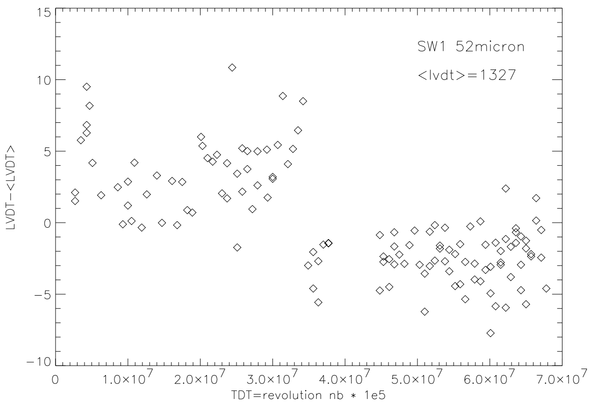

Figure 1. Deviation of the measured position of the [OIII] line from the average value as a function of time. 40 LVDT (linear variable differential transformer) units correspond to 1 resolution element of the grating. The position of the line is slightly different before and after revolution 346. Between revolutions 378 and 442 no observations were made with the LWS because of a problem with the FP interchange wheel.

2.2. Fabry-Perot Mode

The wavelength calibration of the grating provided the basis for the calibration of the Fabry-Perots, which followed the same principle of getting wavelength markers from observing various lines and interpolating for the scan range between them. An additional complication here was that the parallelism of the FP mirrors had to be optimized as well, and it was discovered that in the long wavelength range the optimum commanded offsets for the mirrors vary with wavelength. This delayed the release of AOT's L03 and L04 which make use of the FP's.

Observing with the FP's means to scan over the spectral profile of the grating, hence the wavelength setting of the grating and its profile must be known with very high accuracy. This is particularly relevant for range scans with the FP's, where several scans at different grating positions have to be matched together. As the grating calibration is not absolutely stable (see section 2.1.), the use of L03 is not recommended for high resolution measurements of a continuum with significant structure on the scale of a grating resolution element. If the continuum is smooth and lines are narrow, however, line fluxes can be determined with an accuracy of 20 percent; the flux of the continuum is then best determined with an L01 AOT.

The calibration of each Fabry-Perot is checked once per week; it shows no systematic variations and is constant within a small fraction of a resolution element (see figure 2). The primary standard used here is the narrow line H II region G0.6-0.6, because its lines are strong and only half as broad as a resolution element of the FP's. Since this source is not visible with ISO all the time, sources with broader or weaker lines like the planetary nebula NGC7027 have to be used as well.

Assuming a FWHM of 11.6 ± 1.3 km/sec for the [OIII] line in G36.3+0.7 (Lockman 1989) the deconvolution of the spectral profile and the line shape gave a resolution of 8200 at 88 μm for the FPL; within its margin of error this agrees with the nominal value of 9559 which was determined before launch.

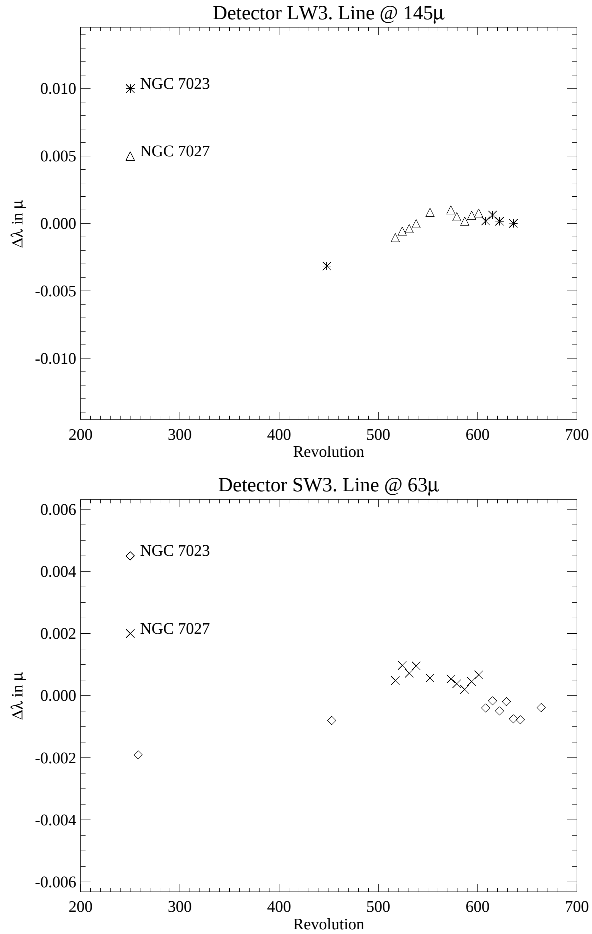

Figure 2. Scatter of measured line positions in FPL (top) and FPS (bottom) as a function of revolution number.

3. FLUX CALIBRATION

The flux calibration is based on end to end grating scans on Uranus with a signal to noise ratio of about 350. The model for Uranus which was used to predict the true flux from that planet rests upon submm observations and has an absolute accuracy of 5 percent for the continuum flux (Griffin & Orton 1993).

It does not include, however, the R(0) and R(1) rotational lines of HD at 112.1 μm and 56.1 μm, respectively, therefore they can appear in emission in the AAR products of observations with very high signal to noise ratio on other targets.
Stars (HR5340 and HR6705), asteroids (Ceres, Pallas and Vesta), Neptune and bright H II regions (G298.228-0.34 and S106) have been observed as well in order to check the calibration on a wide range of fluxes and spectral shapes, to establish secondary standards for the case of Uranus not being visible with ISO and to enable cross-calibration with other instruments on ISO. Their fluxes range from a few Jy to several 10,000 Jy, where saturation of the detectors has to be taken into account. Figure 3 shows the comparison of the AAR from a grating scan on Neptune with a model (Lellouch, priv. comm.); the two are in good overall agreement.

Photometric measurements on standard sources are

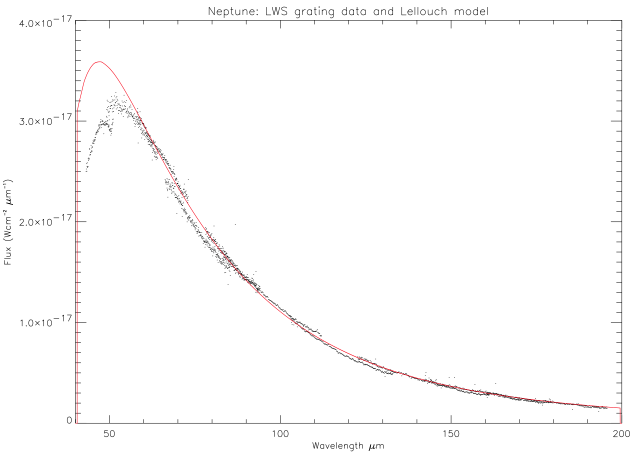

Figure 3. Auto Analysis Result for grating scan on Neptune. The smooth curve gives the flux from the model multiplied by 0.9.

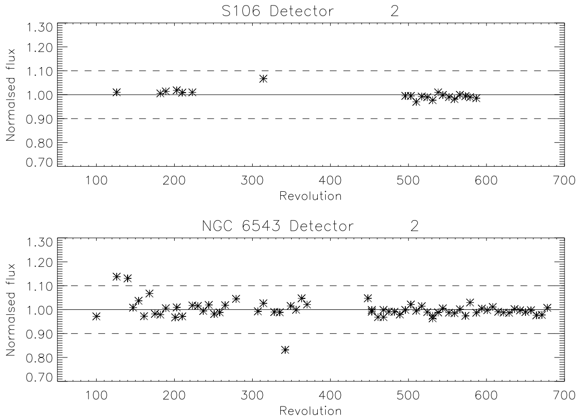

Figure 4. Signal measured in SW3 for a bright H II region and a planetary nebula that were repeatedly observed during the mission.

an essential part of the weekly routine calibration of the LWS until the end of the mission. They have shown that the overall flux varies among end-to-end grating scans by less than ten percent (see figure 4). This result was confirmed by the monitoring of the internal illuminator flashes during handover between ground stations (Burgdorf 1997). High stability was also found for the dark background which is measured as part of every AOT and also during handover. The dark background contributes significantly to the measured signal from a weak source, hence in these cases its deviation from the mean has a direct impact on the photometric accuracy of the measurement.

4. PECULIARITIES OF THE DETECTOR BEHAVIOUR

It was known already before launch that the ionizing radiation to which the detectors are exposed in space causes an increase of responsivity during a revolution (Price 1992), but the most energetic particle hits could not be produced in experiments on the ground. The responsivity is therefore monitored in every AOT with a sequence of standard illuminator flashes. It was found that the responsivity changes with the same linear function of time within the observation window of each revolution. For long scans on strong sources the accuracy of the drift correction is improved by using the signal from the source itself to trace it (Swinyard 1997).
Also the non-linear response to a glitch or a step illuminator change had been investigated already before the mission (Church 1992). One finding was that the transient response is different at the leading edge than at the trailing edge of a step function, therefore the shape of a spectrum measured with the LWS is slightly different for forward and backward scans (Lim 1998). The slow response to changes in illumination is seen clearest in the photometric mode, i e observations with the grating in fixed position (see figure 5). It is therefore recommended to have the observations of this mode lasting at least several minutes, even when a sufficient signal to noise ratio can be achieved earlier. Longer observing times reduce also the susceptibility against big radiation glitches or telemetry drops. Short observations should be compared in interactive analysis with calibration measurements on Uranus.

For sources with fluxes near the upper end of the dynamical range of the instrument the integrated photocurrents at the input nodes of the amplifiers cause a significant drop in the bias voltages across the detectors. The result is that the relationship between infrared flux strength and photocurrent is no longer linear. Observations of Saturn and Mars have been performed to characterize this effect. In order to keep the deviations in the ramp shapes to a minimum a ramp length of only 0.25 sec instead of 0.5 sec is used for sources with fluxes higher than 10^4 Jy.

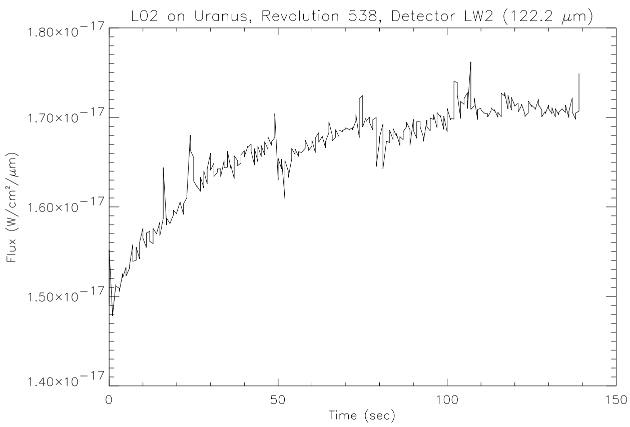

Figure 5. AAR from detector LW2 on Uranus in fixed grating position as a function of time. It shows the transient response that is typical for doped-germanium photoconductors.

5. UNEXPECTED PHENOMENA

5.1. Fringes

Many spectra taken with the grating of the LWS are afflicted by modulations superimposed on the spectrum of the target. These fringes appear only in extended sources and in point sources that are observed off-axis; for sources with a diameter of less than 6 arcsec in the center of the beam they are not detectable. Their properties were characterized with grating scans of Uranus and Mars at different positions in the field of view, and it was found that their period is always 3.6 cm^{-1}. As their amplitude depends on the strength of the source and its position in the beam, a range scan over several periods of the modulation is needed to determine their contribution in a given observation.

5.2. Beam Size

When analyzing the raster observations on planets it was found that the beam size of the LWS in grating mode is smaller than the optical models predicted; this discrepancy is particularly large for longer wavelengths. Table 1 gives first estimates from measurements on Mars which confirmed the values calculated earlier from observations on Uranus. They were derived directly from the normalized beam profiles as measured at the different positions of the raster.

5.3. Infrared Leak

LWS spectra of hot sources, e g stars, sometimes contain broad spurious features. They are identified as false because they do not occur at the same wavelength in different detectors which cover the same range (see figure 6). As the strength of these features is well correlated with the flux of the sources in the H-band, a near-infrared leak in the blocking filters located in front of the detectors is the most likely explanation for the spurious lines. A zero-magnitude source at H, i e F(1.65) = 1050 Jy, gives for example a feature with peak flux 1.5×10^{-18} W $m^{-2} \mu m^{-1}$ in detector SW2. Fitting Gaussians with the values in table 2 removes effectively the spurious features and makes the detection of narrow emission lines at their place possible.

Table 1. Measured beam size for the LWS (full width at half maximum)

Wavelength	Width (y-axis)	Width (z-axis)
μm	arcsec	arcsec
46.1	81	71
56.2	80	77
66.1	82	84
75.7	81	80
84.8	84	76
102.5	78	70
122.2	78	75
141.8	69	65
160.6	72	70
178.0	69	69

Table 2. Position and width of spurious features from hot sources. The values for SW1 and SW3 are less secure, because the bump lies for them mostly outside the spectrum.

Detector	Wavelength	FWHM
	μm	μm
SW2	53.60	1.86
LW1	105.08	4.30
LW2	109.39	3.91
SW1	51.7	2.38
SW3	52.2	3.96

6. DATA PROCESSING

6.1. Pipeline

An observer will normally start the analysis of his observation with the pipeline products SPD or AAR. The automatic processing leads via the following steps from raw data to Standard Processed Data (for further details see the ISOLWS Data Users Manual, SAI/95-219/Dc, by N. Trams):

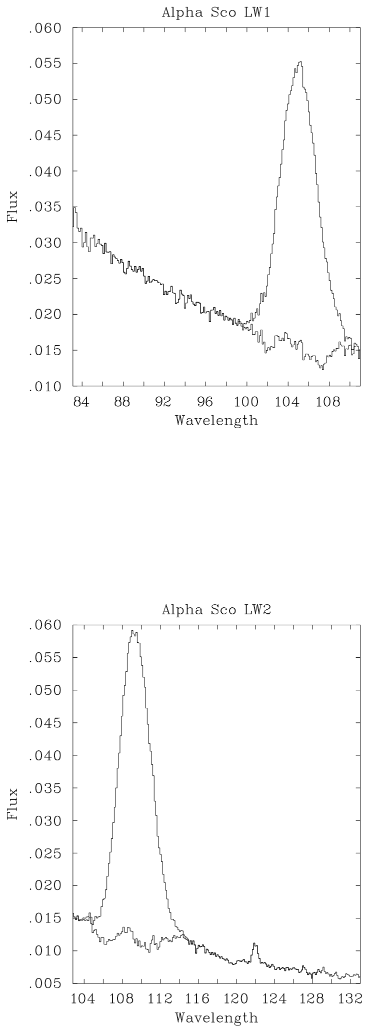

Figure 6. Spectrum of Antares in two detectors where filter leaks are apparent. The spectrum after removal of a fitted Gaussian is overplotted.

- Construction of ramps and discarding the parts that are disturbed by the reset pulse or are saturated.
- Deglitching
- Extraction of ramp slopes and uncertainties. In version 6 of the pipeline the signal current is calculated by fitting a first or second order polynomial to each ramp, depending on its height and length. As there were sometimes discontinuities when the processing switched from one order to the other, version 7 of the pipeline will use a new algorithm for the ramp fitting. It will calculate the slopes from the first and the last point of a second order fit to each ramp.
- Illuminator processing

SPD can only be interpreted by expert users, because its scientific data are still in engineering units. In auto analysis the following processing steps apply then inter alia wavelength and flux calibration:

- Dark background subtraction. The sum of dark current and signal from possible internal straylight is measured every time at the beginning and the end of an AOT. It changed very little over the duration of the mission, so its average value is known with very high accuracy. It is currently under investigation whether subtracting this average value of the dark current instead of the ones measured in the AOT's would reduce the statistical error of the fluxes.
- Scan wavelength calibration - this will be made time dependent for the grating in the new version of the pipeline in order to allow for the sudden jump in revolution 346 (see section 2.1.).
- Spectral responsivity calibration
- Absolute responsivity correction and responsivity drift correction (the latter is not done for measurements in fixed grating position). A correction for strong sources, where debiasing of the detectors causes non-linearities (see section 4.), is planned for a future version of the pipeline. Figure 7 shows how this processing step will restore the shape of a spectrum that is distorted because of a too strong source flux.

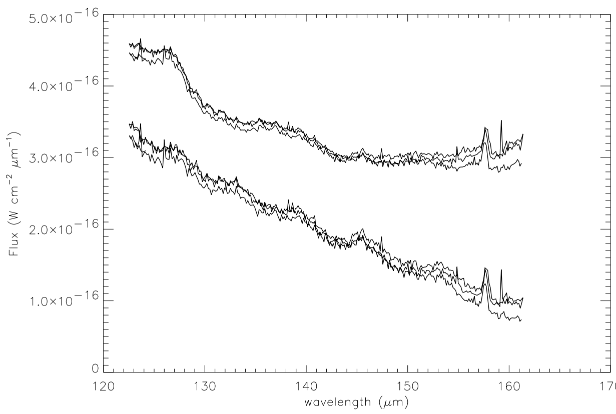

Figure 7. AAR of a strong source (NGC6334) before (top) and after (bottom) correction for non-linearities near saturation in detector LW3. The three scans of that observation have not been averaged.

6.2. ISAP

Although the AAR from the pipeline produces reliable scientific results, the observer usually wants to process his data further, e g in order to average the repeated scans within an AOT, to subtract a background measurement or the like. For this purpose ISAP was developed, a stand alone software package in IDL. Two new routines available in version 1.3 are particularly relevant for solving problems mentioned above:

- ISAP contains the new LWS defringing software for L01. It consists of a program written by

Chris Lloyd at RAL which simultaneously fits a quadratic continuum and a sine wave whose amplitude varies linearly with the wavenumber. Figure 8 shows an LWS spectrum before and after applying the defringing software.

- It is possible to add an offset to the spectrum of a given detector so that the observer can decide himself which dark current value he wants to use (see section 6.1.). Besides, he can use a multiplicative shift in order to modify the responsivity drift correction that is made in the pipeline and which often fails to match the spectra of different detectors together.

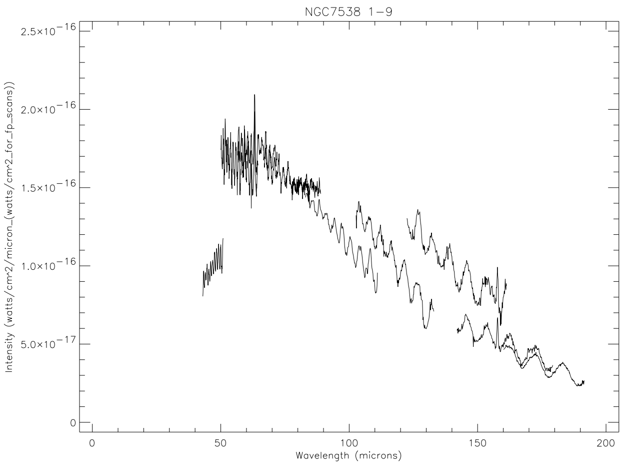

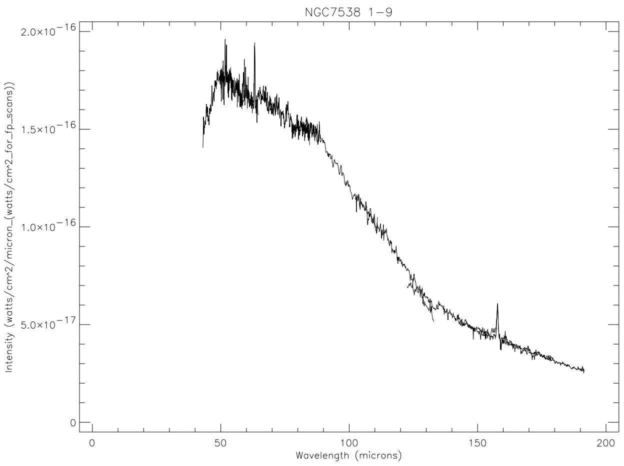

Figure 8. An extended source with strong fringes in the spectrum, before (top) and after (bottom) applying the defringing algorithm and stitching the different detectors together.

6.3. LIA

The LWS Interactive Analysis allows the LWS data user to inspect his pipeline products from different processing stages and enables him to manipulate the contents of the AAR files. The most important functionalities of the LIA are routines for responsivity correction and dark current subtraction; for details see the paper by S. Sidher in these proceedings.

7. CONCLUSIONS

All observing modes of the LWS are routinely used. Wavelength and flux calibration have remained stable and were influenced only very little by a period of several weeks without LWS observations. Therefore monitoring the performance of the instrument has become the main purpose of calibration observations. Additional work is needed to characterize the effect of the unexpectedly small beam size on the photometric calibration for extended sources and to remove the grating profile from FP data. Both the automatic pipeline processing and the interactive routines for analyzing the data are constantly refined; these activities will continue in the post-operational phase.

ACKNOWLEDGMENTS

The LWS was designed and built by a consortium of scientists and engineers from Canada, France, Italy, the U K and the U S A. Hardware and software were provided by: Centre d'Etude Spatiale des Rayonnements, Toulouse, France; Istituto de Fisica dello Spazio Interplanetario, Frascati, Italy; Laboratoire Astronomie Spatiale, Marseille, France; Mullard Space Science Laboratory, University College London, Holmbury St Mary, U K; Rutherford Appleton Laboratory, Chilton, U K; Queen Mary and Westfield College, London, U K; University College London, London, U K.

REFERENCES

Burgdorf, M. J. et al. 1997, Proceedings of an ESA Symposium devoted to the FIRST mission, ESA SP-401

Church, S. E. et al. 1992, Proceedings of an ESA Symposium on Photon Detectors for Space Instrumentation, ESA SP-356, 261-264

Clegg, P. E. et al. 1996, A&A, 315, L38-L42

Delettrez, C. et al. 1994, Experimental Astronomy, 4, 213

Griffin, M. J. and Orton, G. S. 1993, Icarus, 105, 537

Lim, T. L. et al. 1998, Proceedings of the first ISO workshop on analytical spectroscopy with SWS, LWS, PHT-S and CAM-CVF, ESA SP-419

Lockman, F. J. 1989, ApJS, 71, 469

Price, M. C. et al. 1992, Proceedings of an ESA Symposium on Photon Detectors for Space Instrumentation, ESA SP-356, 309-312

Sidher, S. D. et al. 1998, Proceedings of the first ISO workshop on analytical spectroscopy with SWS, LWS, PHT-S and CAM-CVF, ESA SP-419

Swinyard, B. M. et al. 1997, Proceedings of an ESA Symposium devoted to the FIRST mission, ESA SP-401